A 4-, 6-, 20-, and 30-GHz-Band Branching Network Using a Multilayer Dielectric Filter for a Satellite Communication Earth Station

SHUICHI SHINDO, ISAO OHTOMO, MEMBER, IEEE, AND MASAKI KOYAMA, MEMBER, IEEE

Abstract—**This paper describes a four-frequency broad-band branching network for transferring microwave (4 and 6 GHz)- and millimeter-wave (20 and 30 GHz)-band signals between an antenna and transmitter–receivers in a satellite communication earth station. A filter for separating the microwave band from the millimeter-wave band employs a multilayer dielectric filter with matching layers and is included in the primary antenna feed system. The design method used for the multilayer dielectric filter and the construction and experimental results of the four-frequency broad-band branching network are described. Measurements show that its insertion loss, VSWR, and axial ratio are less than 1.2, 1.2, and 2.1 dB, respectively.**

I. Introduction

A JAPANESE domestic satellite communication system has been proposed by the Nippon Telegraph and Telephone Public Corporation [1]. This system is characterized by the simultaneous use of four frequency bands, 4, 6, 20, and 30 GHz. The use of microwave bands (4 and 6 GHz) as well as of millimeter-wave bands (20 and 30 GHz) increases the feasibility of the communication systems.

The ratio of the lowest to the highest frequency is about 8 for the system under consideration. On the other hand, the ratio is 2 or 3 at most for conventional microwave communication systems (4–6 GHz) and millimeter-wave communication systems (40–120 GHz). This fact indicates extreme difficulty in realizing the hardware for antenna and branching network. Especially, the conventional waveguide branching network is not likely to be applicable, because many higher order modes of the millimeter-wave bands will propagate in the branching network and degrade transmission quality.

An early paper reported the feasibility of using the dielectric filter for the satellite communication earth station [2]. In this paper, strict specification of a four-frequency-band branching network, required for application in a practical system, is considered in the operational bandwidths of 0.5 GHz for 4- and 6-GHz bands, and of 3.5 GHz for 20- and 30-GHz bands. This antenna and branching network, combined with a feed system, is composed of the usual Cassegrain antenna, several beam reflectors, a wide-band dielectric filter, and exclusively designed micro- and millimeter-wave primary horns and band diplexers.

Manuscript received May 4, 1976; revised July 26, 1976.

The authors are with the Yokosuka Electrical Communication Laboratory, Nippon Telegraph and Telephone Public Corporation, Yokosuka-shi, 238-03, Japan.

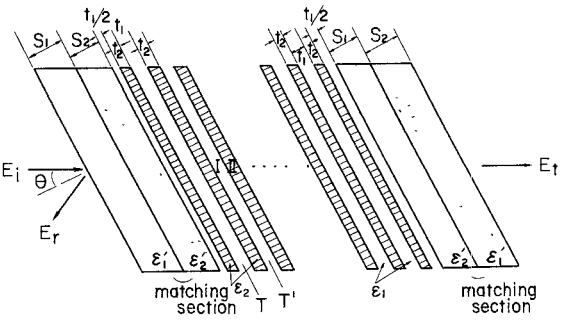

Fig. 1. Multilayer dielectric filter.

This antenna and branching network is 1) free from unwanted higher modes, 2) has low loss, 3) is ultrabroad band, and 4) is flexible in system fabrications.

The following reports on the design method for the multilayer dielectric filter, construction, and experimental results of the four-frequency-band branching network.

II. Design Method for Multilayer Dielectric Filter

Some examples of the application of the multilayer dielectric filter have been shown [3], [4]. Here, the design method is based on the image parameter method. Fig. 1 shows such a filter, utilizing two kinds of dielectric plates. *Ei*, *Er*, and *Et* denote, respectively, the incident wave, the reflected wave, and the transmitted wave. Quantities ε_1 and ε_2 are the relative permittivities of the two different dielectric plates and t_1 and t_2 are their thicknesses; ε_1' and ε_2' are the relative permittivities of the matching dielectric layers and s_1 and s_2 are the thicknesses of the matching layers.

Now, in general, the reflection and transmission at the multilayer dielectric plates are equivalent to the reflection and transmission of the waveguide mode by multilayer dielectric plates placed orthogonally in a waveguide [5]. Assuming lossless dielectrics, propagation constants within dielectric plates I and II are given by

$$\beta_1 = \frac{2\pi}{\lambda_0}\sqrt{\varepsilon_1}\cos\theta \qquad \text{(in I)} \tag{1}$$

$$\beta_2 = \frac{2\pi}{\lambda_0}\sqrt{\varepsilon_2 - \varepsilon_1 \sin^2\theta} \qquad \text{(in II)} \tag{2}$$

where λ_0 is wavelength in the free space and θ is the angle of incidence. When the electric field is parallel to the plane of incidence (called the E wave), the characteristic impedance is given by

$$Z_1^e = Z_0 \cos\theta/\sqrt{\varepsilon_1} \tag{3}$$

within I and by

$$Z_2^e = Z_0\sqrt{\varepsilon_2 - \varepsilon_1 \sin^2\theta/\varepsilon_2} \tag{4}$$

within II. Here $Z_0 = \sqrt{\mu_0/\varepsilon_0}$. Considering the $T - T'$ section of Fig. 1 as a symmetrical two-port network, its image impedance Z_i^e and image propagation constant θ_i^e are given by

$$Z_i^e = Z_1^e \sqrt{\frac{(1-\Omega^2)\omega + (Z_2^e/Z_1^e - Z_1^e/Z_2^e \cdot \omega^2)\Omega}{(1-\Omega^2)\omega + (Z_1^e/Z_2^e - Z_2^e/Z_1^e \cdot \omega^2)\Omega}} \tag{5}$$

$$\theta_i^e = \text{arc cosh}\left[\frac{1}{(1+\omega^2)(1+\Omega^2)} \cdot \{(1-\omega^2)(1-\Omega^2) - 2(Z_1^e/Z_2^e + Z_2^e/Z_1^e)\omega\Omega\}\right] \tag{6}$$

where

$$\omega = \tan\left(\frac{\beta_1 t_1}{2}\right) \tag{7}$$

$$\Omega = \tan\left(\frac{\beta_2 t_2}{2}\right). \tag{8}$$

When (7) and (8) are the same, i.e., when

$$t_2 = \frac{\varepsilon_1}{\varepsilon_2} \cdot \frac{\cos\theta}{\sqrt{1 - \varepsilon_1/\varepsilon_2 \cdot \sin\theta}} \cdot t_1, \qquad \omega = \Omega \tag{9}$$

then (5) and (6) reduce to

$$Z_i^e = Z_1^e \sqrt{\frac{1 - \omega^2 + Z_2^e/Z_1^e - Z_1^e/Z_2^e \cdot \omega^2}{1 - \omega^2 + Z_1^e/Z_2^e - Z_2^e/Z_1^e \cdot \omega^2}} \tag{10}$$

$$\theta_i^e = \text{arc cosh}\left[\frac{1}{(1+\omega^2)^2} \cdot \{(1-\omega^2)^2 - 2(Z_1^e/Z_2^e + Z_2^e/Z_1^e)\omega^2\}\right]. \tag{11}$$

Setting $\theta_i^e = \alpha_i^e + j\beta_i^e$, we obtain 1) when $0 < \omega^2 < Z_2^e/Z_1^e$ and $Z_1^e/Z_2^e < \omega^2$,

$$\alpha_i^e = 0$$

$$\cos\beta_i^e = \frac{1}{(1+\omega^2)^2} \cdot [(1-\omega^2)^2 - 2(Z_1^e/Z_2^e + Z_2^e/Z_1^e)\omega^2]$$

and 2) when $Z_2^e/Z_1^e \le \omega^2 \le Z_1^e/Z_2^e$

$$\cosh\alpha_i^e = \pm\frac{1}{(1+\omega^2)^2} \cdot [(1-\omega^2)^2 - 2(Z_1^e/Z_2^e + Z_2^e/Z_1^e)\omega^2]$$

$$\beta_i^e = n\pi, \qquad n = 1,2,3,\cdots.$$

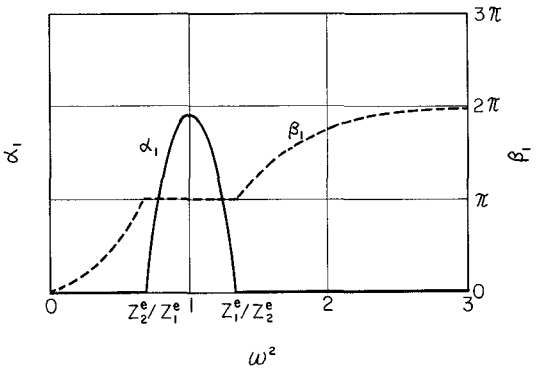

Fig. 2. Angular frequency versus components of image propagation constant.

These relations are shown in Fig. 2. In other words, the multilayer dielectric filter has bandpass characteristics wherein $Z_2^e/Z_1^e \le \omega^2 \le Z_1^e/Z_2^e$ in the reflection range. Otherwise, there is a transmission range.

Similarly, when the electric field is normal to the plane of incidence (called the H wave), the characteristic impedance within dielectric plates I and II is given by

$$Z_1^h = Z_0/\sqrt{\varepsilon_1}\cos\theta \tag{12}$$

$$Z_2^h = Z_0/\sqrt{\varepsilon_2 - \varepsilon_1 \sin^2\theta}. \tag{13}$$

Image parameters are obtained by replacing e with h in (5), (6), (10), and (11).

When the angle of incidence is not zero, then Z_1^e/Z_2^e and Z_1^h/Z_2^h will be different. Hence θ_i^e and θ_i^h are also different. In satellite communication, where there is no fixed polarizing surface or where circular polarization is used, θ_i^e and θ_i^h should be made equal. Thus we set

$$Z_1^e/Z_2^e = C^2 \cdot Z_1^h/Z_2^h. \tag{14}$$

Then, from (3), (4), (12), and (13), we obtain

$$C = \frac{t_2}{t_1} \cdot \frac{1}{\sqrt{\alpha}} \tag{15}$$

where

$$\alpha = \varepsilon_1/\varepsilon_2 \tag{16}$$

or

$$\alpha = \csc^2\theta - \cot^2\theta/C^2. \tag{17}$$

The preceding relation is plotted in Fig. 3 with θ as a parameter. In the figure, λ_c/λ_h (λ_c is the cutoff wavelength corresponding to $\omega^2 = Z_1^e/Z_2^e$ and λ_h is the free-space wavelength corresponding to center frequency of reflection range) and actually utilized dielectric materials are also shown (with $\varepsilon_1 = 1$). As is seen from the figure for a given C, in order to have a wide bandwidth it is necessary to use materials of high permittivity with a small angle of incidence. If materials of low permittivity are used, the bandwidth will become narrow with a large angle of incidence. For the satellite communication filter C should be more than 0.9.

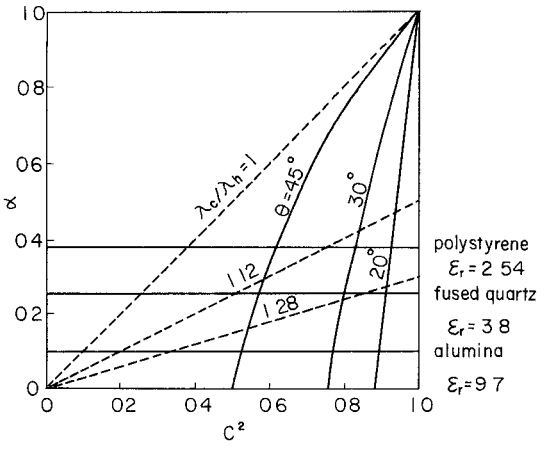

Fig. 3. C^2 ($= Z_1^e Z_2^h / Z_2^e Z_1^h$) versus α ($= 1/\varepsilon$).

Design Example

A multilayer dielectric filter meeting the following specifications is desired: relative permittivities $\varepsilon_1 = 1$ (air) and $\varepsilon_2 = 9.7$, center frequency of reflection range $f_h = 24$ GHz, reflection attenuation over 45 dB by image parameter, and $C = 0.95$ ($\theta = 20°$).

First, from (3), (4), (12), and (13) we obtain $Z_2^e/Z_1^e = 0.3396$ and $Z_2^h/Z_1^h = 0.3036$. Thus the reflection attenuation P_{LE} and P_{LH} per section for E and H waves are

$$P_{LE} = 8.686 \times \text{arc cosh } [(0.3396 + 1/0.3396)/2]$$
$$= 9.38 \text{ dB}$$

and

$$P_{LH} = 8.686 \times \text{arc cosh } [(0.3036 + 1/0.3036)/2]$$
$$= 10.35 \text{ dB}.$$

Then, in order to obtain more than 45-dB attenuation, it is necessary to use 5 sections ($5 \times 9.38 = 46.9$ dB). Letting f_h be the point of $\omega = 1$, we obtain $t_1 = 3.32$ mm and $t_2 = 0.99$ mm.

III. Construction of the Branching Network

Fig. 4 shows the construction of an antenna and four-frequency-band branching network combined with feed system. The primary antenna feed system is composed of well-known beam waveguide with three ellipsoidal reflectors and two corrugated horns for the microwave and the millimeter-wave bands. The dielectric filter is located at the common focal point of three beam reflectors, and the corrugated horns are placed at the other focal points. First, the frequency band 4–6 GHz is separated from 20–30 GHz by the dielectric filter. Then, using second-stage band diplexers, 4 GHz is separated from 6 GHz and 20 GHz is separated from 30 GHz.

The wide-band dielectric filter described here is composed of multilayer dielectric plates designed as reported in the previous section and obliquely with respect to the incident waves. This dielectric filter is designed so that the millimeter wave is reflected obliquely from its surface and the microwave is transmitted through it. Thus the microwave and millimeter-wave bands are independently fed by each

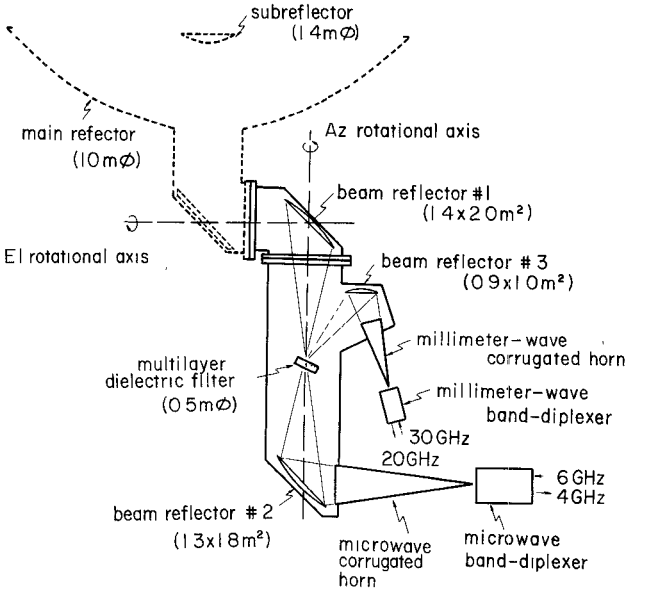

Fig. 4. Construction of antenna and four-frequency-band branching network combined with feed system for satellite communication earth station.

TABLE I
Materials of the Multilayer Dielectric Filter

SECTIONS	KINDS OF DIELECTRIC	RELATIVE * PERMITTIVITIES	tan δ *	THICKNESSES(mm)
MATCHING	TWO FOAMED QUARTZ PLATES **	$\varepsilon_1' = 1.7$	5×10^{-4}	$S_1 = 10.83$
	TWO QUARTZ PLATES	$\varepsilon_2' = 3.8$	1×10^{-4}	$S_2 = 7.10$
MAIN	FIVE ALUMINA PLATES	$\varepsilon_2 = 9.7$	1×10^{-4}	$t_2 = 0.99$
	SIX LAYERS OF AIR (QUARTZ SPACERS)			$t_1 = 3.32$

* Experimental values measured at 38.9 GHz.
** Emerson & Cuming, Inc., ECCOFOAM Q-R.

corrugated horn. The band diplexers are composed of transmit–receive filters to separate transmitted signals (6 and 30 GHz) from received ones (4 and 20 GHz), circular polarizers to convert a linear-polarized wave to a circular one, and a TM_{01} mode coupler to track a satellite. The transmit–receive filter for each band is constructed by a slot-coupled-type coupler with reflecting metal plate.

For the design of the branching network, the following four points are particularly taken into consideration.

1) A beam waveguide composed of two ellipsoidal reflectors is designed for microwave and millimeter-wave bands, such that the radiation patterns of 30 GHz from 4 GHz have the same beamwidths at the subreflector plane.

2) Dielectric materials of the filter are carefully selected to operate for the high-power transmitted signals for the up link (6 and 30 GHz), as shown in Table I.

3) Since the dielectric filter is installed obliquely, the two orthogonally polarized waves have different reflection and transmission coefficients. Therefore, deterioration of the desired circular polarization can occur. To avoid this effect, the optimum incident angle has been chosen. Moreover, it was attempted to reduce the phase difference between the two orthogonally polarized waves.

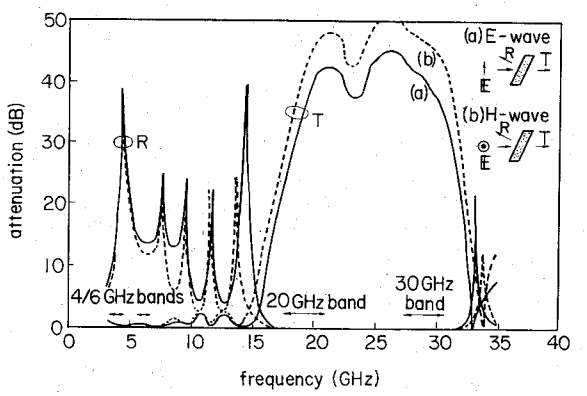

Fig. 5. Theoretical characteristics of the multilayer dielectric filter with matching sections ($\varepsilon_1 = 1$, $\varepsilon_2 = 9.7$).

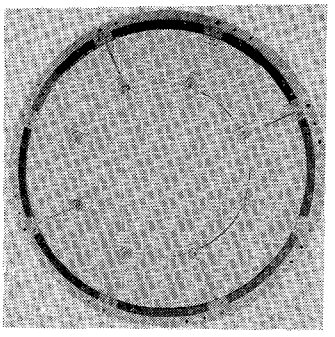

Fig. 6. 500-mm$^{\phi}$ multilayer dielectric filter.

4) The dielectric filter has matching sections, in order to reduce undesired reflection of the microwave bands, that consist of two kinds of dielectric plates. The design is shown in the Appendix.

Fig. 5 shows the theoretical transmission characteristics of the multilayer dielectric filter. The incident angle θ of the dielectric filter is 20°. This filter consists of a five-layer main section with a center frequency of 24 GHz in the stopband, and of two-layer matching sections with a center frequency of 5.5 GHz in the passband. Alumina plates and quartz spacers are piled up alternately in the main section, and solid quartz and foamed quartz are stacked in the main section. No change in dielectric constants of these materials was observed over a temperature range of up to 500°C. Theoretical curves were calculated from the conventional F-matrix method. The main section is designed to satisfy the stopband attenuation of over 25 dB and the matching transformer sections to give equal-ripple characteristics in the passband.

IV. Experimental Results

Figs. 6 and 7 show the multilayer dielectric filter and overall view of the four-frequency-band branching network, set up for indoor experiments. Four kinds of radiation patterns at an equivalent subreflector plane are measured at a distance of about 6 m from beam reflector no. 1. A measuring pickup horn is moved along the x and y axes for E and H waves as shown in Fig. 8. The radiation patterns of the E wave are shown in Fig. 8. They have nearly the same beamwidth from 4 to 30 GHz. H-wave patterns

TABLE II
Overall Transmission Characteristics of the Four-Frequency-Band Branching Network

FREQUENCY (GHz)	4	6	20	30
OPERATIONAL BANDWIDTH (GHz)	0.5 (3.7-4.2)	0.5 (5.925-6.425)	3.5 (17.7-21.2)	3.5 (27.5-31.0)
INSERTION LOSS (dB) *				
BEAM WAVEGUIDE	0.3	0.3	0.3	0.4
DIELECTRIC FILTER	0.7	0.6	0.1	0.1
BAND-DIPLEXER	0.2	0.2	0.7	0.5
(TOTAL)	1.2	1.1	1.1	1.0
VSWR OF INPUT PORT OF BAND-DIPLEXER	1.1	1.2	1.2	1.2
AXIAL RATIO (dB)	0.7	0.8	2.1	2.0

* Theoretical values include losses of corrugated horn, feedome, spillover, and surface roughness of beam reflectors.

are also in good agreement with the E-wave patterns at every frequency. By way of an example, the comparison of E- and H-wave patterns at 4 and 20 GHz is shown in Fig. 9. The radiation patterns of the y axis for E and H waves have nearly the same beamwidth and are similar to the patterns of the x axis at every frequency.

A waveguide phase shifter was constructed using multihole arrays in the axial direction of a circular waveguide, in order to compensate for the phase difference of the dielectric filter between the two orthogonally polarized waves. This results in the axial ratio being below 0.8 dB for the microwave bands and 2.1 dB for the millimeter-wave bands. It shows that the phase difference is reduced to half of the value without the phase shifters.

Table II shows the overall characteristics of the four-frequency-band branching network measured between reflector no. 1 and the band diplexer. The overall insertion loss is below 1.2 dB for the microwave bands and 1.1 dB for the millimeter-wave bands, in agreement with the theoretical values. These measured values include the insertion losses of the dielectric filter, 0.7 dB for the microwave bands and 0.1 dB for the millimeter-wave bands. The latter loss was measured by placing a metal plate at the same focal point. These losses caused the absorption of dielectric tan δ and, for the microwave bands, the scattering from the quartz spacers are in agreement with the theoretical values.

Finally, to examine the characteristics of TM_{01} mode propagation from the corrugated horn to beam reflector no. 1, the difference was measured between the maximum points of the main beam radiation pattern and the null points of the TM_{01} mode radiation pattern at 4 and 20 GHz. These differences were less than 1/20 of the -3-dB beamwidth. It is so small that the accuracy in tracking the satellite may be sufficiently maintained.

V. Conclusion

The 4-, 6-, 20-, and 30-GHz-band branching network, using a multilayer dielectric filter, has successfully been constructed. It is concluded that this branching network

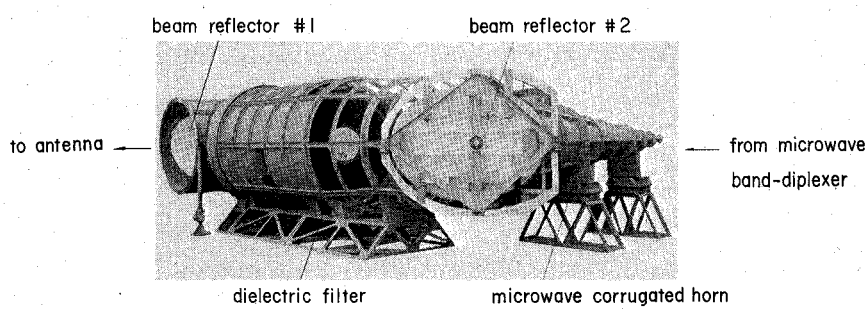

Fig. 7. Overall view of the four-frequency-band branching network combined with feed system.

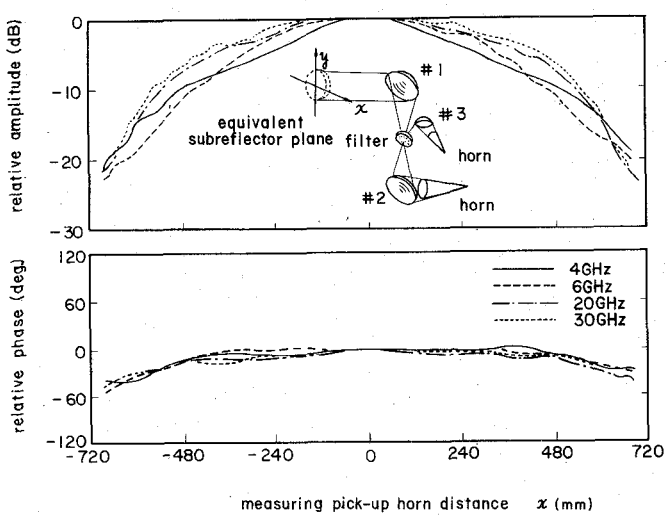

Fig. 8. Radiation pattern frequency characteristics at an equivalent subreflector plane (E wave).

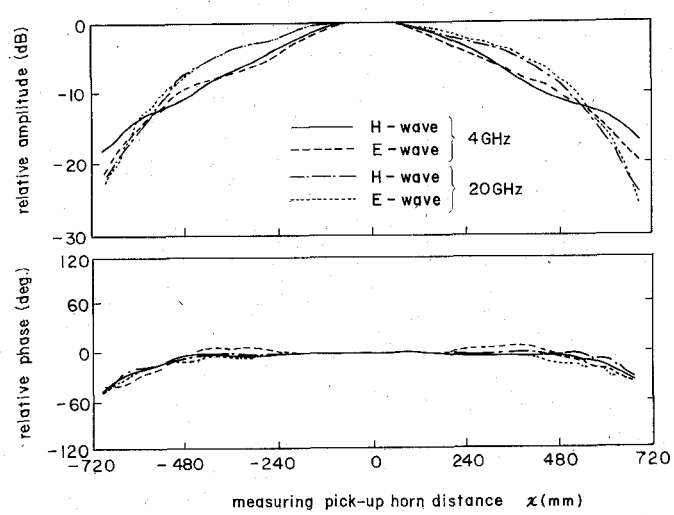

Fig. 9. Radiation pattern E/H-wave characteristics at an equivalent subreflector plane (4 and 20 GHz).

has low loss and broad-band characteristics, and can be applied to various antenna systems for use in future satellite communications systems. Because the microwave-band axial ratio is very low, this network can be applied to the two independently polarized waves to reuse the satellite communication frequency bands.

Appendix

In passbands (4 and 6 GHz), there is about 1-dB fluctuation of the transmitted wave for the E wave and about 1.5 dB for the H wave. Since this is directly related to the transmission loss for these bands, this fluctuation must be reduced. For instance, it is possible to design a Chebyshev filter [6], but this cannot be practical unless many kinds of dielectrics are utilized. Thus the method of adding matching dielectric layers in front and back using two kinds of dielectrics layers was chosen. This new design method is described in the following.

The first step is to design an impedance transformer which transforms the free-space impedance (assuming 1 Ω) into the image impedance of a multilayer dielectric filter at the center frequency of the transmission range. This transformer can be realized with dielectric materials in general. Letting ω_p be the center frequency, then, from (10), the ratio of transformation is given by

$$1:R = \sqrt{\frac{1 - {\omega_p}^2 + Z_2/Z_1 - Z_1/Z_2 \cdot {\omega_p}^2}{1 - {\omega_p}^2 + Z_1/Z_2 - Z_2/Z_1 \cdot {\omega_p}^2}} \quad \text{(A1)}$$

where Z_1/Z_2 is the ratio of the characteristic impedance of the E or H wave. Choosing a two-stage Chebyshev transformer [7], characteristic impedances ${Z_1}^{(m)}$ and ${Z_2}^{(m)}$ of the matching layers are given by

$${Z_1}^{(m)} = \left[\sqrt{\frac{(R-1)^2}{4\tan^2\phi} + R + \frac{R-1}{2\tan^2\phi}}\right]^{1/2} \quad \text{(A2)}$$

$${Z_2}^{(m)} = R/{Z_1}^{(m)} \quad \text{(A3)}$$

where

$$\cos\phi = \cos\phi_c/\sqrt{2} \quad \text{(A4)}$$

and ϕ_c is the electrical length corresponding to bandwidth. The size of the Chebyshev ripple is given by

$$K = \pm\frac{1-R}{4R}\cdot\frac{2-{W_c}^2}{2W_c}, \qquad W_c = \cos\Phi \quad \text{(A5)}$$

where Φ is the electrical length of the matching layers. The values of ${\varepsilon_1}'$ and ${\varepsilon_2}'$ of Fig. 1 can be determined by ${Z_1}^{(m)}$ and ${Z_2}^{(m)}$.

ACKNOWLEDGMENT

The authors wish to thank Dr. S. Shimba, Dr. S. Shimada, and Dr. M. Shinji of the Yokosuka Electrical Communication Laboratory, Nippon Telegraph and Telephone Public Corporation, for their valuable discussions, and the members of the Mitsubishi Electric Corporation for their endeavors in manufacturing this network.

REFERENCES

[1] F. Ikegami and S. Morimoto, "Plans for the Japanese domestic satellite communication system," 1972 IEEE INTERCON.
[2] M. Koyama and S. Shimada, "The quasi-optical filters used for the domestic satellite communication system," *Trans. Inst. Electron. Commun. Eng. of Japan*, vol. 56-B, no. 3, pp. 115–122, March 1973.
[3] J. T. Taub and J. Cohen, "Quasi-optical waveguide filters for millimeter and submillimeter wavelengths," *Proc. IEEE*, vol. 54, no. 4, pp. 647–656, April 1966.
[4] L. Young and E. G. Cristal, "Low-pass and high-pass filters consisting of multilayer dielectric stacks," *IEEE Trans. Microwave Theory Tech.*, vol. MTT-14, no. 2, pp. 75–80, Feb. 1966.
[5] G. R. Schineller, "Variable optical double prism attenuator with multi-wavelength spacing," *Proc. Symp. Quasi-Optics*, Polytechnic Press, Brooklyn, NY, pp. 517–531, 1961.
[6] L. Young, "Synthesis of multiple anti-reflection films over a prescribed frequency band," *Jour. Opt. Soc. America*, vol. 51, no. 9, pp. 967–974, Sept. 1961.
[7] R. E. Collin, "Theory and design of wideband multisection quarter-wave transformers," *Proc. IRE*, vol. 43, no. 2, pp. 179–185, Feb. 1955.

The High-Power *X*-Band Planetary Radar at Goldstone: Design, Development, and Early Results

ROB HARTOP AND DAN A. BATHKER, SENIOR MEMBER, IEEE

Abstract—**Selected critical microwave components for a 400-kW very-long-pulse (several hours) *X*-band radar system are discussed from theoretical and practical viewpoints. Included are the special-sized waveguide and flanges, hybrid power combiner, couplers, switches, polarizer, rotary joints, feedhorn, and radome. The system is installed on the National Aeronautics and Space Administration/Jet Propulsion Laboratory 64-m-diam reflector antenna at Goldstone, CA.**

I. INTRODUCTION

THE 64-m-diam antenna at Goldstone, CA (Fig. 1), operated by the Jet Propulsion Laboratory (JPL) for the National Aeronautics and Space Administration [1], is equipped with a rotatable asymmetric hyperboloidal subreflector that permits the use of multiple feed systems at the Cassegrain focus. The subreflector can be precision indexed to a fixed number of positions (presently five) to allow each feed to properly illuminate the main reflector. Proper illumination is here defined to mean that each feed, in turn, produces a spherical phase front emanating from the prime focus, indistinguishable from that of a perfectly symmetric feed system except for minor amplitude illumination imbalance. Because the spherical phase fronts from the various feeds are not degraded, perfect axial pointing of the overall system is maintained among the feeds and no paraboloid "scan loss" is incurred; the minor amplitude imbalance inherent in this multiple feed system does cause a negligible (< 0.01-dB) illumination loss. In addition, two of the feeds are capable of simultaneous operations through a dual-reflector system consisting of a dichroic plate and ellipsoidal reflector; these two feeds typically operate simultaneously when the hyperboloid is indexed for the dichroic plate position [2].

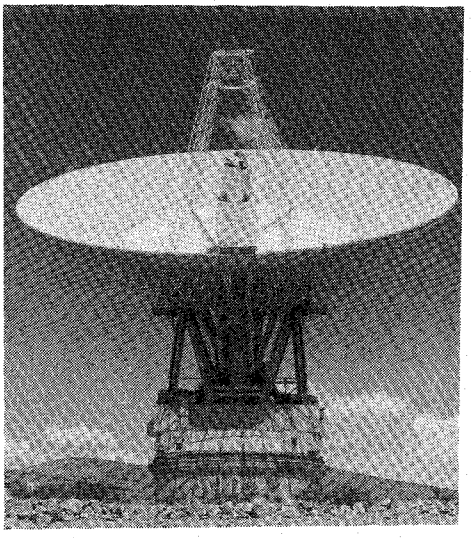

Fig. 1. The 64-m-diam antenna at Goldstone, CA.

For *S*-band frequencies, the feed that operates through the ellipsoidal reflector (Fig. 2) is diplexed for simultaneous

Manuscript received May 17, 1976; revised August 2, 1976. This work was supported by the National Aeronautics and Space Administration under Contract NAS 7-100. This paper presents the results of one phase of research carried out at the Jet Propulsion Laboratory, California Institute of Technology, Pasadena, CA.

The authors are with the Jet Propulsion Laboratory, California Institute of Technology, Pasadena, CA 91103.